Multi-objective design and analysis of a novel extractive distillation configuration with vapor recompression for bioethanol recovery

Juan José Alonso-Tijerina[a], Alejandro Hernández-Magallanes[b], Salvador Tututi-Ávila[c] and Eduardo González-Mora[d]

[a] Universidad Autónoma de Nuevo León, San Nicolás de los Garza, México, juan.alonsotjr@uanl.edu.mx
[b] Universidad Autónoma de Nuevo León, San Nicolás de los Garza, México, javier.hernandezmg@uanl.edu.mx,
[c] Universidad Autónoma de Nuevo León, San Nicolás de los Garza, México, salvador.tututivl@uanl.edu.mx, CA
[d] Universidad Autónoma del Estado de México, Toluca, México, egonzalezmo@uaemex.mx

Abstract:
Distillation operations are responsible for approximately 4% of global energy consumption. Extractive distillation is widely used for bioethanol dehydration due to the ethanol–water azeotrope; however, it is inherently energy intensive because of high reflux ratios and solvent regeneration requirements. Consequently, process intensification and optimization are pivotal for mitigating energy demands, environmental footprints, and associated economic costs. This work investigates the multi-objective optimization of intensified extractive distillation configurations for anhydrous ethanol production. Two intensification strategies are considered: vapor recompression (VRC), which upgrades the latent heat of the overhead vapor to supply the reboiler duty, and thermal coupling through a side rectifier (SR) which replaces a reboiler with a vapor-liquid interconnection. Four configurations are analyzed: conventional extractive distillation (ED-C), thermally coupled extractive distillation (ED-SR), vapor recompression extractive distillation (ED-VRC), and a hybrid configuration integrating both strategies (ED-VRC-SR). Process simulations were performed in Aspen Plus using the NRTL thermodynamic model. A Python–Aspen ActiveX interface was implemented to enable automated multi-objective optimization using the Non-dominated Sorting Genetic Algorithm II (NSGA-II) algorithm. The optimization simultaneously minimizes the Total Annual Cost (TAC) and the environmental impact quantified by the Eco-indicator 99 (EI99). The results of this study highlight the progressive benefits of each intensification strategy relative to the conventional baseline. The ED-C scheme yielded reductions of 8.5% in TAC and 13.1% in EI99. The ED-SR configuration demonstrated enhanced performance, reducing TAC and EI99 by 23.9% and 26.8%, respectively. Furthermore, the ED-VRC scheme achieved a 25.3% decrease in TAC and a substantial 57.7% reduction in EI99. Ultimately, the hybrid ED-VRC-SR configuration delivered the best overall performance, reducing TAC and EI99 by 31.3% and 60.5%, respectively. These findings underscore the potential of hybrid intensification strategies to drive the transition toward more sustainable and economically viable bioethanol production processes.

Keywords:
Extractive Distillation; NSGA-II; Process Intensification; Side Rectifier; Vapor Recompression.

1. Introduction

Ethanol production utilizes diverse feedstocks, with sugar fermentation standing out as one of the most established biotechnological pathways. To be utilized as a fuel, ethanol must adhere to rigorous purity standards, typically exceeding a mass fraction of 99% [1]. Consequently, mixtures obtained from fermentative processes must undergo intensive separation and purification stages prior to commercialization or end-use. A primary challenge in ethanol purification is the formation of a minimum-boiling azeotrope with water. Azeotropic mixtures, comprising two or more components, are characterized by simultaneous evaporation and condensation at a constant composition across both phases, rendering conventional distillation ineffective. In the context of anhydrous ethanol production, extractive distillation (ED) and azeotropic distillation emerge as the predominant separation technologies. Extractive distillation is based on the addition of a selected separation agent, or extractive solvent which exhibits differential physicochemical interactions with the original components, modifying their relative volatilities and thereby facilitating the separation of close-boiling or azeotropic compounds [2].

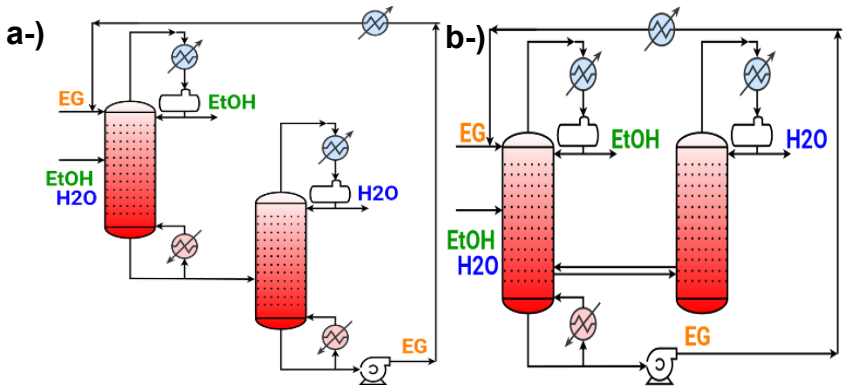

Figure. 1. *a-) Conventional extractive distillation system (ED-C), b-) Extractive distillation system with thermal coupling based on a system with side rectifier (ED-SR).*

Despite its efficacy, extractive distillation is inherently energy-intensive due to the high reflux ratios, the subsequent energy required to recover the solvent in a secondary regeneration column and its high boiling point. This thermal demand often translates into high operational costs and a significant carbon footprint. Process intensification strategies have therefore attracted considerable attention to reduce the energy consumption and environmental impact of distillation-based separations. In this context, two promising approaches are vapor recompression (VRC) and thermal coupling between distillation columns. VRC operates as a heat-pump system by compressing the overhead vapor and reusing its latent heat as the heating source for the reboiler, thereby significantly reducing external steam requirements [3]. Thermal coupling, on the other hand, improves the internal integration of mass and energy through side rectifiers or side strippers. This strategy replaces either a reboiler (side rectifier) or a condenser (side stripper) with a vapor-liquid interconnection [4].

The baseline extractive distillation configuration and the thermally coupled system with a side rectifier are illustrated in Figure 1. The conventional extractive distillation sequence (ED-C) represents the reference configuration typically employed in industrial ethanol dehydration. In contrast, the thermally coupled configuration (ED-SR) incorporates a side and eliminates a reboiler, thereby reducing the overall energy demand of the separation system. Furthermore, Figure 2 illustrates both extractive distillation schemes integrated with VRC. The first intensified configuration (ED-VRC) couples a VRC system with an intermediate heat exchanger, while the second (ED-VRC-SR) employs a synergistic approach by combining VRC with an intermediate heat exchanger and a thermally coupled side rectifier.

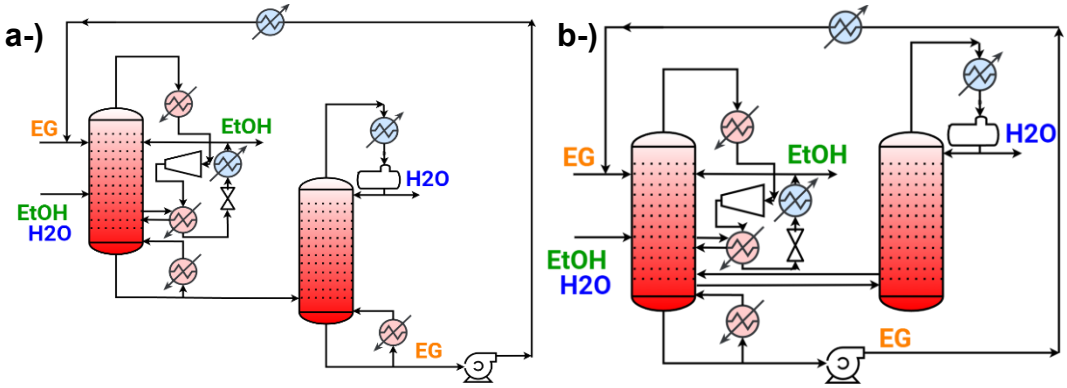

Figure. 2. *a-) VRC assisted extractive distillation system (ED-VRC), b-) VRC assisted extractive distillation system thermally coupled to a side rectifier (ED-VRC-SR).*

Recent literature emphasizes the synergy between multiple intensification strategies to overcome the high energy demands of extractive distillation. Aurangzeb et al. (2019) demonstrated that while an Extractive Dividing Wall Column (EDWC) alone achieves 13.6% energy saving, its integration with Vapor Recompression (VRC) significantly boosts performance, reaching a 54.2% reduction in energy consumption and a 30.4% decrease in Total Annual Cost (TAC) compared to conventional sequences [1]. Similarly, Wang et al. (2021) reported that VRC implementation can reduce steam-related costs by up to 83.4% and CO_2 emissions by 26.9%, highlighting VRC as a primary driver for both economic and environmental sustainability [5]. Li et al. (2021) evaluated various thermal coupling arrangements for the separation of benzene-isopropanol-water, concluding that an extractive column integrated with a side rectifier represents the optimal design for this

specific system. This configuration yielded a 32.8% reduction in CO_2 emissions and a 28.7% saving in TAC [6].

Although vapor recompression and thermally coupled distillation have been studied individually, their combined implementation within extractive distillation systems with intermediate heat exchangers has received limited attention in the literature, particularly from a multi-objective optimization perspective considering both economic and environmental performance. Therefore, this research focuses on the multi-objective optimization (MOO) of four intensified extractive distillation configurations for anhydrous ethanol production, specifically targeting the simultaneous minimization of the Total Annual Cost (TAC) and the Eco-indicator 99 (EI99). By establishing a conventional separation sequence as a benchmark, this study evaluates the synergistic potential of Vapor Recompression (VRC) and side-stream rectifiers (SR) to navigate the complex trade-offs between economic viability and environmental stewardship. The optimization framework employs a metaheuristic approach with the Non-dominated Sorting Genetic Algorithm II (NSGA-II) to explore the high-dimensional design space including both operational and design variables inherent to each distillation column scheme.

2. Methodology

The extractive distillation configurations considered in this study (ED-C, ED-SR, ED-VRC, and ED-VRC-SR), previously introduced in Figures 1 and 2, were simulated and optimized following the methodology described in the next sections.

2.1. Process simulation

All process simulations were performed using Aspen Plus V14 to ensure rigorous thermodynamic modeling of the extractive distillation process. The Non-Random Two-Liquid (NRTL) model was selected to describe the non-ideal vapor–liquid equilibrium behavior of the ethanol–water–ethylene glycol system, while distillation columns were modeled using the RADFRAC module. The feed stream consisted of 100 kmol h^{-1} of an ethanol–water mixture containing 84 mol% ethanol, while 100 kmol h^{-1} of ethylene glycol (EG) was used as the extractive solvent. All columns were assumed to operate close to atmospheric pressure with a pressure drop of 0.0068 bar per stage. These operating conditions resulted in condenser temperatures compatible with cooling water utilities and reboiler duties requiring high-pressure steam. The conventional configuration was first optimized to establish a reference design, which was subsequently used to evaluate the intensified configurations.

2.2. Multi-objective optimization framework

The optimization of the distillation configurations was formulated as a multi-objective optimization problem aimed at simultaneously minimizing economic and environmental objectives. The optimization was performed using the Non-dominated Sorting Genetic Algorithm II (NSGA-II). An automated computational framework was implemented by coupling Python with Aspen Plus through an ActiveX interface, allowing the optimization algorithm to iteratively modify process variables, execute simulations, and evaluate objective functions. The NSGA-II algorithm was implemented using a population size of 500 individuals, 50 generations, a crossover rate of 0.8, and a mutation rate of 0.05 based on the work of Tututi et al. (2014) [7]. The optimization simultaneously minimizes the following objective functions:

$$\min \mathrm{TAC}(\mathbf{x}) \quad (1)$$

$$\min \mathrm{EI99}(\mathbf{x}) \quad (2)$$

Where **x** represents the vector of decision variables.

Capital cost (CapEx) correlations for the main equipment were estimated using standard cost relationships from the work of Douglas [8]. Utility prices were taken from the work of Turton et al. to calculate operational costs (OpEx) [9]. Three utility costs have been considered: high-pressure steam (42 bar, 254 °C, \$17.7/GJ), cooling water (\$0.72/GJ), and electricity (\$16.8/GJ). The operating costs were evaluated by 8500 h of operation per year. The Total Annual Cost (TAC) includes both annualized capital costs and operating expenses, assuming a 10-year payback period. Correlation costs are the following:

$$\mathrm{ColumnCost} = 17640(\mathrm{D})^{1.066}(\mathrm{L})^{0.802}\ ; \mathrm{D},\ \mathrm{L}\ (\mathrm{m}) \quad (3)$$

$$\mathrm{CondenserCost} = 7269(\mathrm{A})^{0.65}\ ;\ \mathrm{U} = 0.852\,\frac{\mathrm{kW}}{\mathrm{K\,m^2}}\ ;\ \mathrm{A}\ (\mathrm{m^2}) \quad (4)$$

$$\mathrm{ReboilerCost} = 7269(\mathrm{A})^{0.65}\ ; \mathrm{U} = 0.568\,\frac{\mathrm{kW}}{\mathrm{K\,m^2}}\ ;\ \mathrm{A}\ (\mathrm{m^2}) \quad (5)$$

$$\mathrm{CompressorCost} = 5840(P)^{0.82}\ ;\ \mathrm{P}\ (\mathrm{kW}) \quad (6)$$

Where D and L represent column diameter and height, A is the heat-transfer area, and P is the compressor power.

The Total Annual Cost (TAC) is calculated as:

$$\mathrm{TAC} = \frac{\mathrm{CapEx}}{\text{Payback period}} + \mathrm{OpEx} \qquad (7)$$

Product purity constraints (in mass fraction) and recovery (in mole flow) were imposed to ensure process feasibility:

$$\mathrm{X\,EtOH} \geq 0.995 \quad (8)$$

$$\mathrm{X}\,H_2\mathrm{O} \geq 0.995 \quad (9)$$

$$\mathrm{X\,EG} \geq 0.995 \quad (10)$$

$$\mathrm{F_{EtOH}} \geq 0.995\,\mathrm{A_{EtOH}} \quad (11)$$

$$\mathrm{F}_{EG} \geq 0.995\,\mathrm{A_{EG}} \quad (12)$$

2.3. Environmental impact assessment

The environmental performance of each configuration was evaluated using the Eco-indicator 99 (EI99) methodology, which aggregates life-cycle environmental impacts into a single score expressed in milli-points (mPt). The method evaluates environmental damage in three main categories: human health, ecosystem quality, and resource depletion [10]. In this study, the hierarchist cultural perspective (H/H) was adopted. It considers environmental issues with a medium time-horizon (typically 100 years), representing a pragmatic balance between proven short-term issues and more speculative long-term effects. In the standard Hierarchical weighting set (H/H), Human Health and Ecosystem Quality are typically weighed as equally important, while Resource Depletion is given a lower weight. Environmental impacts were calculated considering the contributions associated with steel usage in equipment construction, steam consumption, and electricity demand during plant operation.The scale of the values considered in Table 1 is chosen such that the value of 1 point is representative for a 1000th of the yearly environmental load of one average European inhabitant as in the work of G. Contreras et al. (2019) [11].

Table 1. *Values of EI99 Impact Categories Used for Distillation Columns [10] [11].*

Impact Category	Steel (points/kg) ×10−3	Steam (points/kg)	Electricity (points/kWh)
Carcinogens	1.29×10^{-3}	1.180×10^{-4}	4.360×10^{-4}
Climate change	1.31×10^{-2}	1.27×10^{-3}	4.07×10^{-3}
Ionizing radiation	4.510×10^{-4}	1.91×10^{-6}	8.94×10^{-5}
Ozone layer depletion	4.550×10^{-6}	7.78×10^{-7}	5.41×10^{-7}
Respiratory effects	8.010×10^{-2}	1.56×10^{-3}	1.01×10^{-5}
Acidification	2.710×10^{-3}	1.21×10^{-4}	9.88×10^{-4}
Ecotoxicity	7.450×10^{-2}	2.85×10^{-4}	2.14×10^{-4}
Land occupation	3.730×10^{-3}	8.60×10^{-5}	4.64×10^{-4}
Fossil fuels	5.930×10^{-2}	1.24×10^{-2}	1.01×10^{-2}
Mineral extraction	7.420×10^{-2}	8.87×10^{-6}	5.85×10^{-5}

The Eco-indicator 99 (EI99) is calculated as:

$$\mathrm{EI99} = \sum_i \omega \mathrm{c_i as} + \sum_i \omega \mathrm{c_i asl} + \sum_i \omega \mathrm{c_i ael} \qquad (13)$$

Where ω is a weighting factor for damage, c_i is the value of impact for category i, “as” is the amount of steam utilized by the process, “asl” is the amount of steel used to build the equipment, and “ael” is the electricity required by the process.

The decision variables include both continuous variables (such as reflux ratios, flow rates, and compressor pressure) and discrete variables (such as feed stage locations and interconnection stages). These problems were formulated as a retrofit of a conventional extractive distillation scheme into more intensified configurations. This is evidenced by maintaining fixed values for column diameter, height, and the total number of stages during the optimization of the ED-SR, ED-VRC, and ED-VRC-SR schemes. The complete set of decision variables considered for each configuration is summarized in Table 2.

Table 2. *Decision variables for each configuration.*

Decision variables	ED-C	ED-SR	ED-VRC	ED-VRC-SR
Discrete variables				
Stage number D-101	X	-	-	-
Stage number D-102	X	-	-	-
Solvent feed stage D-101	X	X	X	X
Mixture feed stage D-101	X	X	X	X
Mixture feed stage D-102	X	-	X	-
Interconnection exit stage	-	X	-	X
Intermediate heat exchanger exit stage	-	-	X	X
Continuous variables				
Distillates rate D-101	X	X	X	X
Distillates rate D-102	X	X	X	X
Reflux ratio D-101	X	X	X	X
Reflux ratio D-102	X	-	X	-
Diameter D-101	X	-	-	-
Diameter D-102	X	-	-	-
Column height D-101	X	-	-	-
Column height D-102	X	-	-	-
Interconnection exit flow	-	X	-	X
Intermediate heat exchanger input flow	-	-	X	X
Superheat degrees	-	-	X	X
Compressor discharge pressure	-	-	X	X
Total decision variables	13	7	11	11

3. Results

The resulting set of non-dominated solutions obtained using the NSGA-II algorithm is presented in Figure 3. As shown in Figure 3, the Pareto frontier reveals a partially aligned relationship between TAC and EI99. In general, reductions in energy consumption led to simultaneous improvements in both economic and environmental performance. This behavior is mainly associated with the reduction in steam consumption, which directly affects the operational component of TAC and the fossil-fuel-related environmental impacts represented in the EI99 metric. From the Pareto frontier, a representative optimal solution was selected based on engineering criteria that prioritize lower operational expenditure while maintaining a reasonable capital investment. This selected solution was used as the reference design for the subsequent evaluation of the intensified configurations.

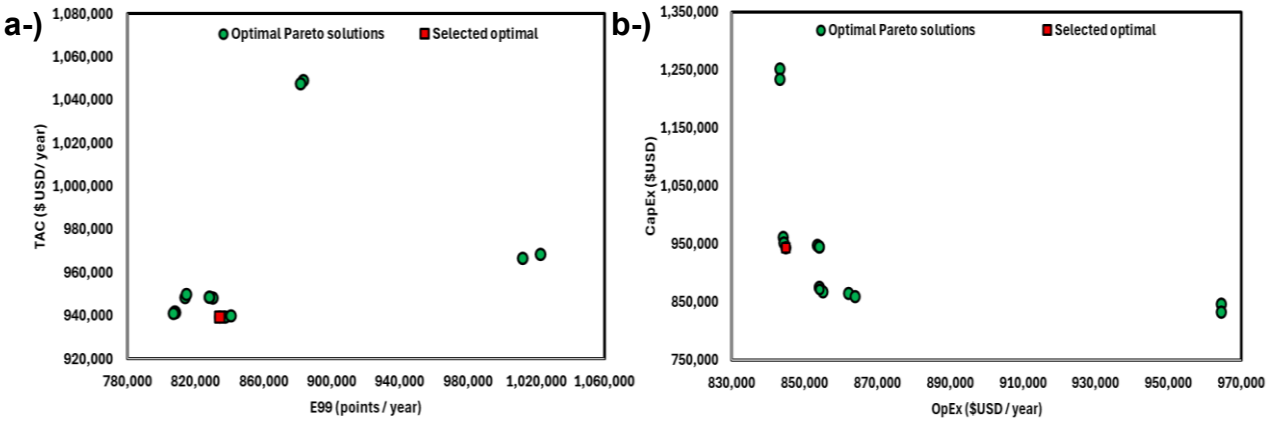

Figure. 3*. a-) Pareto front between TAC and EI99, b-) CapEx vs OpEx.*

The optimal design parameters for each configuration are summarized in Table 3. The inherent advantages of VRC into the distillation sequence are evidenced by the substantial reduction in both heating and cooling thermal loads. Specifically, the optimized ED-VRC scheme achieved a reduction of 66.2% in heating duty and 54.2% in cooling duty compared to the baseline. These results align with existing literature [12,13], which identifies VRC systems as a premier intensification strategy for mitigating external utility requirements.

When thermal coupling is implemented via a side-stream rectifier, the ED-VRC-SR configuration yielded the most significant performance gains, achieving reductions of 69.5% and 57.6% in heating and cooling duties,

respectively. In contrast, the standalone side-stream rectifier scheme (ED-SR) provided a reduction of approximately one-third relative to the most intensified case, with values of 23.1% and 23.2% for heating and cooling, respectively. These findings underscore the superior efficiency of VRC-based intensification, as the revalorization of latent heat effectively displaces the need for external thermal energy. Finally, the conventionally optimized scheme (ED-C-OPT) showed a marginal improvement of 6.7% in both thermal criteria, highlighting the limitations of parametric optimization without structural intensification.

It is noteworthy that the operational parameters for both side-stream rectifier configurations (ED-SR and ED-VRC-SR) exhibit significantly lower reflux ratios in both columns compared to the alternative schemes. Despite this reduction in internal reflux, both intensified designs consistently achieve the target purity specifications, exceeding a mass fraction of 99.5% for each component. However, this gain in energy efficiency and reflux reduction is accompanied by a limitation in separation yield; specifically, the water recovery for both thermally coupled schemes is approximately 88.94%. This suggests that while side-stream rectification optimizes the thermal profile and reduces utility consumption, it introduces a constraint on the total recovery of the secondary component that must be balanced against the achieved energy savings.

Table 3. *Design of four extractive distillation schemes for ethanol dehydration.*

System	ED-C		ED-C-OPT		ED-SR-OPT		ED-VRC-OPT		ED-VRC-SR-OPT	
Column	D101	D102	D101	D102	D101	D102	D101	D102	D101	D102
Stages	22	21	20	15	20	15	20	15	20	15
Feed stage	17	4	15	4	13	15	11	8	10	15
Solvent feed stage	3	-	3	-	3	-	4	-	3	-
Interconnection stages	-	-	-	-	18/15	-	-	-	17/15	-
Interconnection flowrate (kmol/h)	-	-	-	-	15.94	-	-	-	17.2	-
Intermediate heat exchanger exit stage	-	-	-	-	-	-	14	-	13	-
Intermediate heat exchanger input flow (kmol/h)	-	-	-	-	-	-	237.1	-	233.74	-
Bioethanol flowrate (kmol/h)	84	0.15	84	0.007	84	0.02	84	0.004	84	0.014
Water flowrate (kmol/h)	16	15.98	16	15.98	16	14.25	16	15.84	16	14.23
EG flowrate (kmol/h)	100	99.9	100	99.95	100	99.92	100	99.98	100	99.99
Bioethanol purity (wt.%)	99.95		99.91		99.81		99.93		99.89	
Water purity (wt.%)	99.95		99.83		99.54		99.56		99.73	
EG purity (wt.%)	99.97		99.95		99.53		99.99		99.55	
Bioethanol recovery (%)	99.82		99.99		99.98		99.99		99.98	
Water recovery (%)	99.87		99.87		89.06		99		88.93	
Reflux ratio	1	1.2	0.823	0.97	0.521	0.162	0.726	0.843	0.666	0.311
Operating pressure (bar)	1	1	1	1	1	1.12	1	1	1	1.12
Column diameter (m)	1.067	0.609	0.85	0.677	0.85	0.677	0.85	0.677	0.85	0.677
Tray spacing (m)	0.609	0.609	0.558	0.533	0.558	0.533	0.558	0.533	0.558	0.533
Discharge pressure (bar)	-	-	-	-	-	-	7.03	-	7.13	-
Compressor power (kW)	-	-	-	-	-	-	347	-	335	-
Q_{SH} (kW) superheater	-		-		-		185		169	
Q_{HX} (kW) cooler	594		610		586		612		587	
QC (kW) condenser	1832	400	1672	353	1399	187	397	284	401	211
Total $Q_{COOLING}$ (kW)	2825		2635		2172		1293		1199	
Q_R (kW) reboiler	2227	596	2094	539	2170	-	296	472	691	-
Total $Q_{REBOILER}$ (kW)	2822		2633		2170		953		860	
Cooling duty savings (%)	0		6.7		23.1		54.2		57.6	
Heating duty savings (%)	0		6.7		23.1		66.2		69.5	

On the other hand, note that the feasibility of doing a retrofit or renovation of a distillation column, from an existent optimized extractive distillation column, towards intensified schemes is feasible in both energetic, operational and productive terms. As seen in Table 3 every scheme proposed achieved the desired purity and recovery of bioethanol while maintaining a high recovery rate for the solvent and the purity necessary for operation.

From an industrial perspective, the technical feasibility of retrofitting an existing optimized extractive distillation unit into the proposed intensified configurations is demonstrated across energetic, operational, and productivity metrics. As evidenced by the results in Table 3, each intensified scheme successfully adhered to the stringent purity and recovery specifications for bioethanol. Furthermore, these configurations maintained the high solvent recovery rates and requisite recycling purities essential for continuous plant operation. This suggests that the structural modifications required for VRC and SR intensified schemes do not compromise the primary separation objectives but rather enhance the global efficiency of the process without sacrificing product integrity.

From an economic perspective, intensified configurations involving VRC inherently demand a higher CapEx due to the integration of specialized equipment, such as mechanical compressors and heat exchangers. However, as illustrated in Figure 4, the substantial reduction in OpEx more than compensates for the initial investment. The VRC-based schemes achieved an OpEx reduction exceeding 45% compared to the conventional baseline (ED-C), a trend primarily attributed to the displacement of high-pressure utility steam through the revalorization of latent heat. The ED-VRC scheme achieved a TAC reduction of 25.3%, while the most intensified configuration, ED-VRC-SR, reached a remarkable reduction of 31.3% relative to the conventional case. In comparison, the thermally coupled ED-SR scheme reduced the TAC by 23.9%; notably, this configuration required the lowest capital investment among the intensified alternatives, making it an attractive option for scenarios with high capital constraints. Finally, the parametric optimization of the conventional system (ED-C-OPT) yielded a modest 8.5% reduction in TAC, highlighting that structural intensification is necessary to achieve significant economic and energetic breakthroughs.

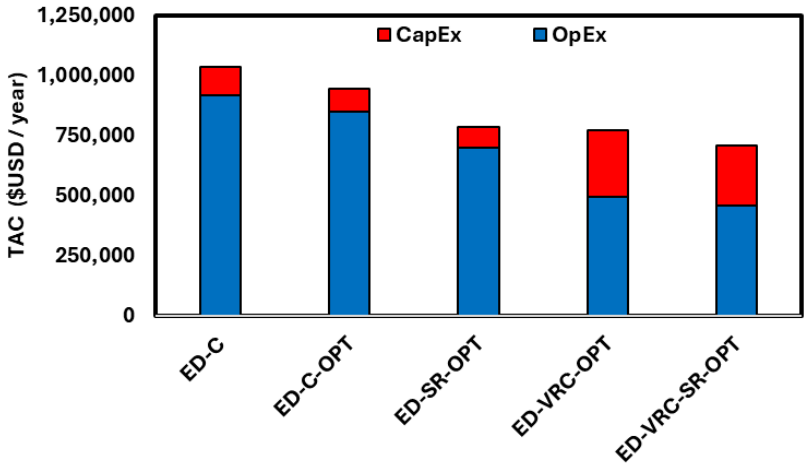

Figure. 4. *Economic performance of each proposed scheme.*

The environmental assessment reveals a significant mitigation of the ecological footprint across all intensified configurations, as shown in Figure 5. The ED-VRC scheme achieved a reduction of 57.7% in EI99 points, a performance gain primarily driven by the drastic reduction in external high-pressure steam requirements enabled by the heat pump integration. Similarly, the most intensified configuration (ED-VRC-SR) yielded a maximum reduction of 60.5%. It is important to highlight that this environmental benefit is intrinsically linked to the energy mix; the impact could be further suppressed by sourcing the compressor's electricity from renewable energy portfolios (e.g., solar or wind), which would nearly eliminate the operational carbon footprint of the intensification unit.

In contrast, the ED-SR configuration reduced the environmental impact by 26.8%, largely through a more modest reduction in thermal duty. The optimization of the conventional case (ED-C-OPT) provided a 13.1% reduction, stemming from simultaneous improvements in column sizing (steel requirements) and steam consumption. A comparative analysis of the results illustrated in Figure 5 indicates that the environmental savings offered by VRC-based schemes are approximately double those achieved by the side-stream rectifier system alone. This disparity underscores that while structural modifications like side-rectifiers are beneficial, the integration of heat-pump-assisted distillation remains the superior pathway for achieving substantial environmental sustainability in bioethanol purification.

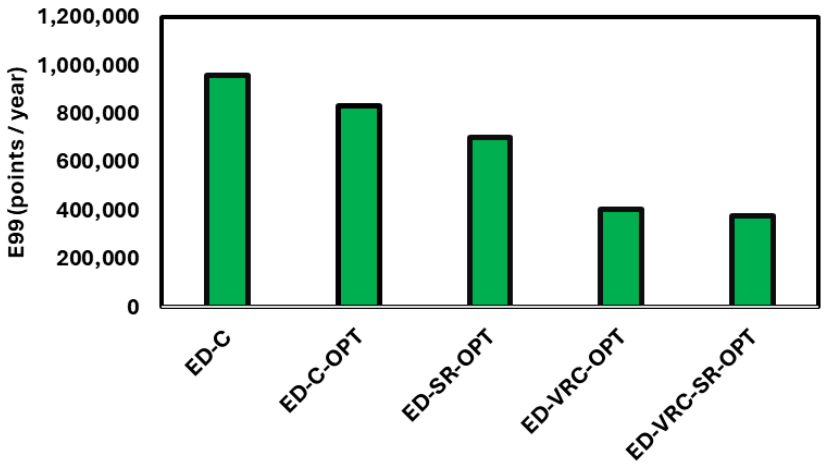

Figure. 5. *Environmental performance of each proposed scheme.*

A detailed analysis of the percentage contributions to the EI99 categories for the optimized conventional (ED-C-OPT) and side-rectifier (ED-SR-OPT) schemes is presented in Figure 6. The results indicate a consistent profile across these configurations, where the consumption of HP vapor emerges as the primary driver of environmental degradation in nearly every category. This dominance underscores that the ecological footprint of extractive distillation is fundamentally an energy-intensive challenge rather than one of material infrastructure. Specifically, the impacts associated with HP vapor are most pronounced in human health-related categories, including Carcinogens, Respiratory effects, and Climate change, as well as the depletion of Fossil fuels. In contrast, the environmental impact of Steel, while significantly lower overall, is uniquely concentrated in the Mineral extraction category, reflecting the primary resource demands of column fabrication.

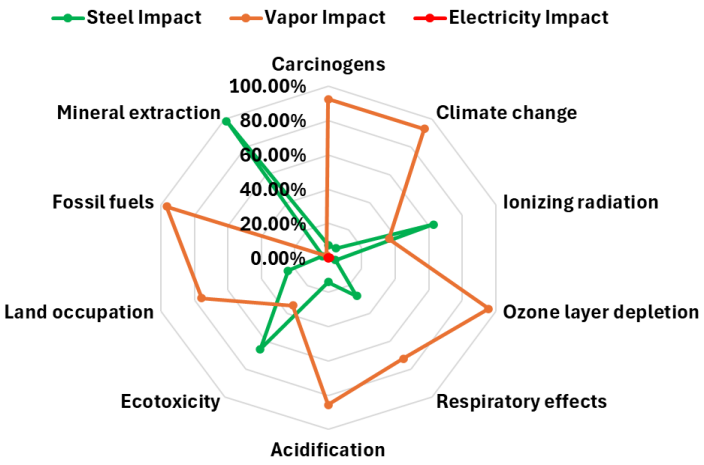

Figure. 6. *Environmental percentage contribution per impact category: ED-C-OPT and ED-SR-OPT.*

The shift in environmental contribution for the intensified VRC schemes is detailed in Figure 7. A comparison with the non-intensified baseline reveals that the integration of a heat pump mechanism drastically alters the process's environmental profile. By substituting high-pressure vapor with mechanical compression, there is a substantial reduction in the percentage contributions across all categories previously dominated by steam consumption, most notably in Fossil fuels, Climate change, and Respiratory effects. While the reliance on HP vapor is significantly mitigated, the Electricity impact emerges as a more prominent factor in this configuration, particularly within the Ionizing radiation and Acidification categories. However, the overall reduction in total EI99 points, previously discussed, confirms that the environmental cost of the electricity required for compression is far lower than the impact of the steam it displaces. Furthermore, the contribution of Steel remains localized to Mineral extraction and Ecotoxicity due to the nature of the optimization problem but does not create a disproportionate environmental burden compared to the massive gains in operational sustainability. This redistribution highlights the synergistic benefit of VRC in extractive distillation, where the revalorization of latent heat acts as a powerful lever for cross-category environmental mitigation.

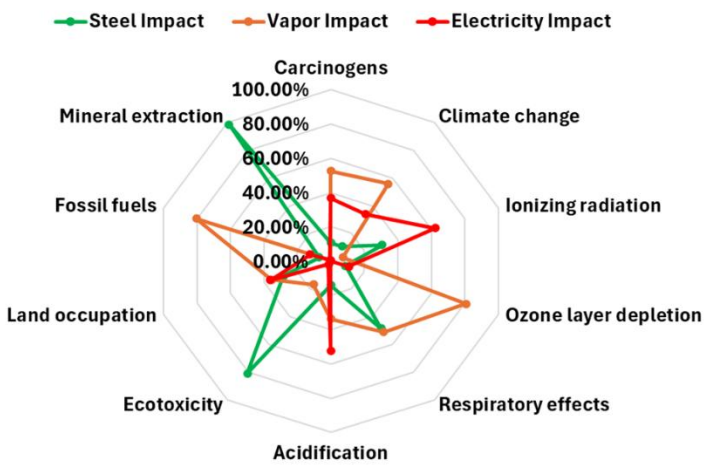

Figure. 7. *Environmental percentage contribution per impact category: ED-VRC-OPT and ED-VRC-SR-OPT.*

4. Conclusions

This work presented a multi-objective optimization framework for the intensification of bioethanol purification through extractive distillation. Four configurations were evaluated: a conventional extractive distillation system (ED-C), a thermally coupled configuration with a side-stream rectifier (ED-SR), a vapor recompression system (ED-VRC), and a hybrid configuration integrating both strategies (ED-VRC-SR).

The results demonstrate that process intensification significantly improves both economic and environmental performance. While the optimization of the conventional scheme (ED-C-OPT) yielded modest reductions of 8.5% in TAC, 13.1% in EI99, and 6.7% in both heating and cooling duties, the intensified alternatives reached much higher benchmarks. The introduction of thermal coupling in the ED-SR-OPT configuration resulted in a TAC reduction of 23.9% and an environmental mitigation of 26.8%, supported by duty reductions of 23.1% (heating) and 23.2% (cooling). Integration of Vapor Recompression (VRC) represented a major energetic breakthrough. The ED-VRC-OPT scheme achieved a TAC reduction of 25.3% and a drastic EI99 improvement of 57.7%, primarily due to a 66.2% reduction in heating duty and a 54.2% reduction in cooling duty.

However, the most effective performance was achieved by the synergistic ED-VRC-SR-OPT configuration. This scheme reached a 31.3% reduction in TAC and a 60.5% reduction in EI99, supported by duty reductions of 69.5% and 57.6% for heating and cooling, respectively. From an environmental standpoint, the life cycle assessment confirmed that displacing high-pressure steam with mechanical electricity shifts the process burden away from fossil-fuel-intensive categories toward impact categories like ionizing radiation, which can be further mitigated via renewable energy sourcing. Overall, the results demonstrate that combining vapor recompression and thermal coupling is a promising strategy for the development of more sustainable and economically competitive bioethanol purification systems.

Acknowledgments

Juan José Alonso-Tijerina acknowledges the financial support provided by SECIHTI through the graduate scholarship granted for his master's studies, which enabled the development of this research project. Additionally, author Eduardo González-Mora expresses his gratitude to COMECyT for the support provided through the fellowship CAT-0112 within the framework of the AESCo project.

Nomenclature

A heat-transfer area, m^2

ael electricity required by process, kWh

as amount of steam utilized by process, kg

asl amount of steel used for equipment construction, kg

D column diameter, m

F molar flow rate, $kmol/h$

L column height, m

P compressor power, kW

Q thermal load or duty, kW

U overall heat transfer coefficient, $kW/(K \cdot m^2)$

X mass fraction, dimensionless

Greek symbols

ω weighting factor for damage, dimensionless

Subscripts and superscripts

C condenser

EG ethylene glycol

EtOH bioethanol

H2O water

HX heat exchanger

R reboiler

SH superheater

References

[1] Aurangzeb M., Jana A.K., A Novel Heat Integrated Extractive Dividing Wall Column for Ethanol Dehydration. Ind Eng Chem Res 2019;58(21):9109–17.

[2] Aquilon A.F., Cargullo D.M., Onayan J., Sarno J., Molino V.M., Lopez E.C.R., Recent Advances in Extractive Distillation. Eng Proc 2023;56(1):15261.

[3] Kazemi A., Hosseini M., Mehrabani-Zeinabad A., Faizi V., Evaluation of different vapor recompression distillation configurations based on energy requirements and associated costs. Appl Therm Eng 2016;94:305–13.

[4] Tang W.T., Chien C.K., Ward J.D., A review of energy intensification strategies for distillation processes: Cyclic operation, stacking, heat pumps, side-streams, dividing walls and beyond. Sep Purif Technol 2025;357:130030.

[5] Wang C., Zhuang Y., Liu L., Zhang L., Du J., Heat pump assisted extractive distillation sequences with intermediate-boiling entrainer. Appl Therm Eng 2021;186:116511.

[6] Li M. et al., Simulated annealing-based optimal design of energy efficient ternary extractive dividing wall distillation process for separating benzene-isopropanol-water mixtures. Chin J Chem Eng 2021;33:146-160.

[7] Tututi-Avila S., Jiménez-Gutiérrez A., Hahn J., Control analysis of an extractive dividing-wall column used for ethanol dehydration. Chem Eng Process 2014;82:88–100.

[8] Douglas J.M., Conceptual design of chemical processes. New York, USA: McGraw-Hill; 1988.

[9] Turton R., Shaeiwitz J.A., Bhattacharyya D., Whiting W.B., Analysis, Synthesis, and Design of Chemical Processes. 5th ed. Upper Saddle River, USA: Prentice Hall; 2018.

[10] Goedkoop M., Spriensma R., The Eco-Indicator 99: A Damage Oriented Method for Life Cycle Impact Assessment. Amersfoort, Netherlands: PRé Consultants; 2001.

[11] Contreras-Zarazúa G. et al., Inherently Safer Design and Optimization of Intensified Separation Processes for Furfural Production. Ind Eng Chem Res 2019;58(15):6105–20.

[12] Liu X., Luo H., Lei Y., Wu X., Gani R., Heat-pump-assisted reactive distillation for direct hydration of cyclohexene to cyclohexanol: a sustainable alternative. Sep Purif Technol 2022;280:119808.

[13] Liu Z., Hao L., Han X., Cao Z., Wei H., Novel energy saving and economic extractive distillation process via integrating two-feed preheating strategy and heat pump vapor recompression. Sep Purif Technol 2023;307:122791.